(3) Fernández-Santín, J. M.; Aymami, J.; Rodriguez-Galán, A.; Muñoz-Guerra, S.; Subirana, J. A. *Nature (London)* **1984**, *311*, 53-54.
(4) Yuki, H.; Okamoto, Y.; Taketani, Y.; Tsubota, T.; Marubayashi, Y. *J. Polym. Sci., Polym. Chem. Ed.* **1978**, *16*, 2237-2251.
(5) Manning, J. M.; Moore, S. *J. Biol. Chem.* **1968**, *243*, 5591-5597.
(6) Doty, P.; Bradbury, J. A.; Haltzer, A. M. *J. Am. Chem. Soc.* **1956**, *78* 947-954.
(7) Flory, P. J. In *Statistical Mechanics of Chain Molecules*; Wiley: New York, 1969; p 277.
(8) Bradbury, E. M.; Carpenter, B. G.; Stephens, R. M. *Biopolymers* **1968**, *6*, 905-915.
(9) Block, H. *Poly(γ-benzyl L-glutamate) and Other Glutamic Acid Containing Polymers*; Gordon and Breach: New York, 1983.
(10) Bamford, C. H.; Elliott, A.; Hanby, W. E. In *Synthetic Polypeptides*; Academic: New York, 1956; p 157.
(11) Bradbury, E. M.; Elliott, A. *Polymer* **1963**, *4*, 47.
(12) Matsubara, I.; Itoh, Y.; Shinomiya, M. *J. Polym. Sci. Polym. Lett. Ed.* **1966**, *4*, 47-53.
(13) Fraser, R. D. B.; MacRae, T. P. *Conformation in Fibrous Proteins*; Academic: New York, 1973.
(14) Cochran, W.; Crick, F. H. C.; Vand, V. *Acta Crystallogr.* **1952**, *5*, 581.
(15) Bradbury, E. M.; Downie, A. R.; Elliott, A.; Hanby, W. E. *Proc. Roy. Soc London, Ser. A* **1960**, *259*, 110-128.
(16) Kovacs, J.; Ballina, R.; Rodin, R. L.; Balasubramanian, D.; Applequist, J. *J. Am. Chem. Soc.* **1965**, *87*, 119-120.
(17) Campbell-Smith, P. J.; Arnott, S. *Acta Crystallogr., Sect. A* **1978**, *34*, 3-11.
(18) Blundell, T.; Barlow, D.; Borkakoti, N.; Thornton, J. *Nature (London)* **1983**, *306*, 281-283.
(19) Van Holde, K. E. *Physical Biochemistry*; Prentice-Hall: Englewood Cliffs, NJ, 1971; p 216.
(20) Paolillo, L.; Temussi, P. A.; Bradbury, E. M.; Cary, P. D.; Crane-Robinson, C.; Hartman, P. G. In *Peptides, Polypeptides and Proteins*; Blout, E. R., Bovey, F. A., Goodman, M., Lotan, N., Eds.; Wiley-Interscience: New York, 1974; pp 177-189.
(21) Bestian, H. *Angew. Chem., Int. Ed. Engl.* **1968**, *7*(4) 278-285.
(22) Schmidt, E. *Angew Makromol. Chem.* **1970**, *14*, 185-202.

Crystalline Features of 4,4′-Isopropylidenediphenylbis(phenyl carbonate) and Conformational Analysis of the Polycarbonate of 2,2-Bis(4-hydroxyphenyl)propane

Serge Perez† and Raymond P. Scaringe*

Corporate Research Laboratories, Eastman Kodak Company, Rochester, New York 14650.
Received July 18, 1986

ABSTRACT: The crystal structure of a complete structural analogue of poly(oxycarbonyloxy-1,4-phenyleneisopropylidene-1,4-phenylene) (bisphenol A polycarbonate) is reported. The crystal structure results have been used to extract valence geometry information for modeling the polymer, and a full helical parameter analysis of the polymer is reported for the first time. The helical parameter analysis has been supplemented by conformational energy calculations using molecular mechanics methods. It is found that there are only two idealized conformations that are consistent with existing fiber data on the crystalline polymer. Moreover, the calculations suggest that there are only a few conformations suitable to serve as templates for the aggregation of photoconductive pyrylium dyes.

Introduction

Poly(oxycarbonyl-1,4-phenyleneisopropylidene-1,4-phenylene) (bisphenol A polycarbonate (BPAPC)) is reported to form a cocrystalline complex with thiapyrylium salts in solvent-cast thin films.[1] These films exhibit unusually high photoconductivity, which is believed to result from an ordered arrangement of the dye molecules in the complex.[2] The optical spectrum in the region of the dye absorption displays features that are reminiscent of well-known dye aggregates in solution, which has led to the term "aggregate" in reference to the thin-film system. Similar aggregation phenomena may also occur in a number of polymer–small molecule mixtures,[3-5] but structural characterization is generally quite difficult. An unusual amount of detailed, although indirect, structural information is available for the thiapyrylium/polycarbonate aggregate, due to the preparation of single-crystal samples of a model complex in which the polycarbonate is replaced by the dicarbonate 4,4′-isopropylidenediphenylbis(phenyl carbonate) (DPBC). The resulting "model aggregate" structure has been determined by single-crystal X-ray diffraction techniques.[1] Comparison of the X-ray powder diffraction patterns of the two substances provides ample evidence that the structure of the model complex closely resembles that of the actual polymer-based system. This is also consistent with optical studies of the two complexes. Thus, these materials provide an unusual opportunity to examine various aspects of small molecule–polymer interactions at the atomic scale.

Table I
Crystal Data for 4,4′-Isopropylidenediphenylbis(phenyl carbonate)

$C_{29}O_6H_{24}$; MW = 468.5; $F(000)$ = 492 e^{-1}
a = 18.863 (3), b = 6.385 (2), c = 10.556 (2) Å
β = 110.63 (10)°, V = 1189.8 Å; $P2_1$
monoclinic
d_{obsd} = 1.31 Mg m^{-3}, d_{calcd} = 1.308 Mg m^{-3}
M(Mo Kα) = 0.85 mm^{-1}
λ(Mo Kα) = 0.7103 Å
T = 20 °C

A remarkable feature of the model aggregate structure is the extended head-to-tail arrangement of the DPBC molecules, which is analogous to the periodic propagation of a linear polymer in the crystalline phase. This observation prompted us to evaluate, through the use of helical parameter analysis, the conformational properties of polycarbonate chains from the perspective of regular periodic structures. Conformational energy calculations have also been performed to aid in assessing the relative stability of different helical structures. As a preliminary step in

† On sabbatical leave from Centre de Recherches sur les Macromolecules Vegetales, 38042 Saint-Martin d'Heres, France.

0024-9297/87/2220-0068$01.50/0

the analysis, we also determined the crystal structure of DPBC. This is the first report of a detailed structure analysis and the precise dimensions for a complete (i.e., DPBC contains both diphenyl carbonate and diphenyldimethylmethane fragments) low-molecular-weight analogue of BPAPC. The valence geometry information extracted from the crystal structure results has been used extensively in the conformational studies reported here.

Materials and Methods

A. Experimental Procedures. Single crystals of DPBC were obtained by slow evaporation of a methanol–acetone solution. Weissenberg and precession photographs indicated a monoclinic unit cell. The systematic absences ($0k0$, $k \neq 2n$) are compatible with both $P2_1$ and $P2_1/m$ space groups. Further measurements were made on a Picker diffractometer. The unit cell dimensions and their standard deviations (determined by least-squares refinement of 20 carefully centered high-angle reflections) are given in Table I.

Intensity data were collected from a crystal of dimensions 0.20 × 0.20 × 0.55 mm, using a scintillation counter and filtered Mo Kα radiation, for two octants within the sphere limited by $2\theta < 60°$. Peaks were scanned by the θ–2θ technique and with a minimum width of 2°(2θ). Background counts of 20 s were taken at each end of the scan range. The intensity of four reference reflections, monitored every 70 min, did not show any decrease over the duration of the data collection. The data were corrected for Lorentz and polarization effects. Owing to the low value of the absorption coefficient, no absorption correction was applied. Of the 3779 reflections measured, 2486 were kept for the structure resolution and refinement. The reflections have $I/\sigma(I) > 2.0$, where $\sigma(I)$ is estimated from counting statistics.

B. Structure Determination and Refinement. A set of normalized structure factors, E, was obtained after isotropic temperature correction. Analysis of the E statistics strongly indicated a noncentrosymmetric space group. The structure was solved in the noncentrosymmetric space group $P2_1$, using the multisolution method.[6] A phasing model could not be achieved until a full stereochemical model of the structure was used in the calculation of normalized structure factors. The E map, calculated with the best set of phases, revealed the positions of 32 non-hydrogen atoms. The three missing non-hydrogen atoms were located in a subsequent Fourier map.

Structure refinement proceeded smoothly, and all the hydrogen atoms were located on successive difference Fourier maps. In the final cycles, all non-hydrogen atoms were refined anisotropically, while the isotropic thermal parameters of the hydrogen atoms were refined. The function minimized in all refinements was $w(|F_o| - |F_c|)^2$. At the end of the refinement, an extinction coefficient was introduced and refined. Comparison of the observed and calculated structure factors, as a function of structure factor magnitude, scattering angle, and Miller indices, showed that several low-angle reflections exhibited a discernible discrepancy. Therefore, they were omitted from the final refinement cycles. The final residuals calculated for $F_o > 2\sigma$ were $R = 0.051$ and $R_w = 0.044$. At this stage, the average shift-to-error ratio was less than 0.1. A final electron-density map showed no significant residual density, the largest peak being 0.18 e/Å^3. Final positional and thermal parameters are given in Table II.

C. Conformational Analysis. Whereas the crystal structure coordinates of the non-hydrogen atoms were used to derive a mean valence geometry for the monomeric unit of the parent polymer, those of the hydrogen atoms were recalculated based on a C–H distance of 1.10 Å.

The sign of the torsion angles is defined by the rules recommended by the IUPAC–IUB Commission of Biochemical Nomenclature.[7] The torsion angle can take on any value between −180° and +180°. The trans conformation is defined by a value of 180°; conversely, the cis arrangement corresponds to a value of 0°.

The potential energy was calculated by including the contributions arising from the van der Waals interactions and inherent torsion potentials where appropriate. This was performed by using the Lennard-Jones function, $E_{ij} = -a/r^6 + b/r^{12}$, for each pair of interacting atoms i and j, excluding 1–3 interactions. The a and b constants were calculated according to the parameters given by Scott and Scheraga.[8] The energy maps were computed as a function of the variable skeletal torsion angles at fixed intervals (typically 5° and 10°). With respect to the relative energy minimum, isoenergy contours were drawn by interpolation of 1 kcal/mol.

Helical arrangement is customarily described in terms of a set of helical parameters (n, h), n being the number of residues per turn of the helix and h being the translation of the corresponding residue along the helix axis. Whenever the values of $h = 0$ or n

Table II
Table of Positional Parameters and Their Estimated Standard Deviations

atom	x	y	z	B, Å^2
O(1)	0.64235 (9)	0.0028 (3)	0.3075 (2)	4.07 (4)
O(2)	0.5170 (1)	0.002	0.1924 (2)	6.50 (6)
O(3)	0.57471 (9)	−0.2352 (3)	0.3501 (2)	4.09 (4)
O(4)	0.08794 (9)	−0.4613 (5)	−0.2712 (2)	5.55 (6)
O(5)	0.1598 (1)	−0.5638 (4)	−0.3881 (2)	6.62 (6)
O(6)	0.0514 (1)	−0.3894 (4)	−0.4811 (2)	5.69 (5)
C(1)	0.6556 (1)	0.1929 (5)	0.2523 (2)	3.48 (6)
C(2)	0.6250 (1)	0.2381 (6)	0.1173 (3)	4.47 (7)
C(3)	0.6429 (2)	0.4273 (6)	0.0730 (3)	5.67 (8)
C(4)	0.6906 (2)	0.5638 (5)	0.1616 (3)	5.91 (8)
C(5)	0.7218 (2)	0.5143 (6)	0.2954 (3)	5.68 (8)
C(6)	0.7045 (2)	0.3264 (5)	0.3410 (3)	4.73 (7)
C(7)	0.5717 (1)	−0.0686 (5)	0.2733 (2)	3.65 (6)
C(8)	0.5048 (1)	−0.3372 (4)	0.3275 (2)	3.38 (6)
C(9)	0.4827 (1)	−0.4923 (5)	0.2324 (2)	3.98 (6)
C(10)	0.4152 (1)	−0.5931 (5)	0.2125 (2)	3.82 (6)
C(11)	0.3697 (1)	−0.5441 (4)	0.2873 (2)	2.83 (5)
C(12)	0.3954 (1)	−0.3895 (4)	0.3841 (2)	3.09 (5)
C(13)	0.4628 (1)	−0.2862 (4)	0.4046 (2)	3.50 (6)
C(14)	0.2943 (1)	−0.6601 (4)	0.2580 (2)	3.03 (5)
C(15)	0.2425 (1)	−0.6167 (4)	0.1113 (2)	3.08 (5)
C(16)	0.2429 (2)	−0.4232 (5)	0.0538 (3)	4.15 (6)
C(17)	0.1934 (2)	−0.3740 (6)	−0.0747 (3)	4.68 (7)
C(18)	0.1428 (1)	−0.5209 (6)	−0.1452 (2)	4.18 (6)
C(19)	0.1399 (1)	−0.7137 (6)	−0.0937 (3)	4.67 (7)
C(20)	0.1906 (1)	−0.7605 (5)	0.0351 (3)	4.07 (6)
C(21)	0.1066 (1)	−0.4838 (5)	−0.3810 (2)	4.14 (6)
C(22)	0.0595 (1)	−0.3831 (6)	−0.6081 (2)	4.19 (6)
C(23)	0.0827 (2)	−0.2023 (7)	−0.6474 (4)	6.7 (1)
C(24)	0.0855 (2)	−0.1946 (8)	−0.7775 (4)	9.9 (1)
C(25)	0.0676 (2)	−0.361 (1)	−0.8578 (3)	10.6 (1)
C(26)	0.0427 (2)	−0.5353 (9)	−0.8182 (3)	8.4 (1)
C(27)	0.0388 (2)	−0.5485 (6)	−0.6916 (3)	5.51 (8)
C(28)	0.2520 (1)	−0.5852 (5)	0.3496 (2)	4.06 (6)
C(29)	0.3122 (2)	−0.8926 (5)	0.2856 (3)	4.52 (7)
H(2)	0.591 (1)	0.142 (5)	0.062 (2)	5.7 (7)[a]
H(3)	0.621 (1)	0.463 (5)	−0.022 (2)	5.8 (7)[a]
H(4)	0.704 (1)	0.681 (4)	0.130 (2)	4.4 (6)[a]
H(5)	0.756 (1)	0.598 (5)	0.360 (3)	5.8 (7)[a]
H(6)	0.726 (1)	0.292 (4)	0.428 (2)	4.2 (6)[a]
H(9)	0.512 (1)	−0.519 (4)	0.178 (2)	4.6 (6)[a]
H(10)	0.402 (1)	−0.699 (4)	0.147 (2)	3.6 (5)[a]
H(12)	0.366 (1)	−0.354 (4)	0.439 (2)	3.6 (5)[a]
H(13)	0.477 (1)	−0.187 (4)	0.467 (2)	3.5 (6)[a]
H(16)	0.279 (1)	−0.319 (5)	0.101 (2)	5.4 (7)[a]
H(17)	0.194 (1)	−0.243 (5)	−0.118 (2)	4.9 (6)[a]
H(19)	0.105 (2)	−0.812 (5)	−0.141 (3)	7.0 (8)[a]
H(20)	0.191 (1)	−0.900 (5)	0.069 (2)	4.7 (6)[a]
H(23)	0.096 (1)	−0.108 (5)	−0.591 (2)	4.9 (6)[a]
H(24)	0.105 (2)	−0.082 (6)	−0.778 (3)	8.7 (9)[a]
H(25)	0.072 (2)	−0.334 (7)	−0.946 (3)	10 (1)[a]
H(26)	0.031 (2)	−0.662 (8)	−0.873 (4)	11 (1)[a]
H(27)	0.025 (1)	−0.667 (5)	−0.663 (3)	5.7 (7)[a]
H(281)	0.281 (1)	−0.611 (4)	0.441 (2)	3.0 (5)[a]
H(282)	0.207 (1)	−0.662 (5)	0.326 (2)	4.6 (6)[a]
H(283)	0.236 (1)	−0.437 (5)	0.329 (2)	5.9 (7)[a]
H(291)	0.345 (1)	−0.908 (5)	0.378 (2)	5.3 (7)[a]
H(292)	0.331 (2)	−0.962 (6)	0.224 (3)	6.6 (8)[a]
H(293)	0.269 (1)	−0.972 (5)	0.274 (2)	4.4 (6)[a]

[a] Atoms were refined isotropically. Anisotropically refined atoms are given in the form of the isotropic equivalent thermal parameter defined as $(4/3)[a^2B(1,1) + b^2B(2,2) + c^2B(3,3) + ab(\cos\gamma)B(1,2) + ac(\cos\beta)B(1,3) + bc(\cos\alpha)B(2,3)]$.

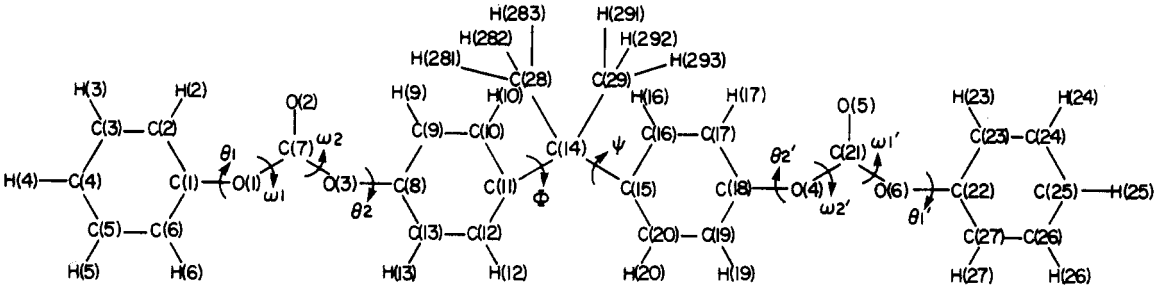

Figure 1. Schematic of 4,4′-isopropylidenediphenylbis(phenyl carbonate) (DPBC) along with the atomic numbering system and the torsion angles of interest.

Table III
Bond Distances (Å) and Their Estimated Standard Deviations

O(1)–C(1) = 1.407 (3)	O(6)–C(22) = 1.402 (3)
O(1)–C(7) = 1.333 (3)	O(6)–C(21) = 1.338 (3)
O(2)–C(7) = 1.172 (3)	O(5)–C(21) = 1.151 (3)
O(3)–C(7) = 1.326 (3)	O(4)–C(21) = 1.332 (3)
O(3)–C(8) = 1.413 (3)	O(4)–C(18) = 1.420 (3)
C(1)–C(2) = 1.367 (3)	C(22)–C(23) = 1.350 (5)
C(2)–C(3) = 1.379 (5)	C(23)–C(24) = 1.392 (10)
C(3)–C(4) = 1.362 (5)	C(24)–C(25) = 1.328 (10)
C(4)–C(5) = 1.362 (5)	C(25)–C(26) = 1.330 (9)
C(5)–C(6) = 1.373 (5)	C(26)–C(27) = 1.366 (6)
C(6)–C(1) = 1.358 (4)	C(27)–C(22) = 1.343 (5)
C(8)–C(9) = 1.366 (3)	C(18)–C(17) = 1.358 (4)
C(9)–C(10) = 1.376 (4)	C(17)–C(16) = 1.385 (4)
C(10)–C(11) = 1.391 (3)	C(16)–C(15) = 1.378 (4)
C(11)–C(12) = 1.380 (3)	C(15)–C(20) = 1.376 (3)
C(12)–C(13) = 1.380 (3)	C(20)–C(19) = 1.392 (4)
C(13)–C(18) = 1.360 (3)	C(19)–C(18) = 1.355 (5)
C(14)–C(11) = 1.535 (3)	C(14)–C(15) = 1.537 (3)
C(14)–C(28) = 1.532 (4)	C(14)–C(29) = 1.527 (4)

= 2 are interchanged, the screw axis of the helix changes to the opposite sense. The chirality of the helix is defined by the sign of n. These parameters were computed following an algorithm reported previously.[9] As already noted by these authors, helical parameters are fully suited to characterize a variety of macromolecular architectures. Among these, two correspond to special cases. The first one is reached for values of $h = 0$, and it corresponds to conformations (impossible for infinite chains) in which the path is circular. The second case corresponds to a macromolecular chain that is made up of monomeric units all related by a pure translation operation. This particular situation will be described by the magnitude of the translation t, instead of the helical parameter h.

Computer programs used in this study include parts of the Enraf-Nonius structure determination package and the Texray refinement package for structural elucidation. The graphic displays were obtained with the aid of a package of interactive computer program systems for plotting molecules and crystal structures.[10,11] A series of interactive computer programs for generating molecules[12] and a general program to calculate the intramolecular energy of a molecule, as well as the helical parameters of the corresponding polymer,[13] were used in the conformational analysis part of this work. All computations were carried out on a PDP 11/23 minicomputer, which is equipped with 512K of RAM and an array processor operating under the Digital Equipment Corporation RSX-11M operating system.

Results and Discussion

A. Conformation and Crystalline Features of DPBC. A schematic of DPBC is given in Figure 1, along with the atomic numbering system and the torsion angles of interest. A view of the DPBC molecule is shown in Figure 2a.

The interatomic bond distances and angles involving the non-hydrogen atoms are listed in Tables III and IV, respectively. The standard deviations of these quantities derived from the calculated estimated standard deviations of the fractional coordinates amount to 0.03 Å for C–H distances and 0.35° for C–C–H angles. The torsion angles of interest are given in Table V.

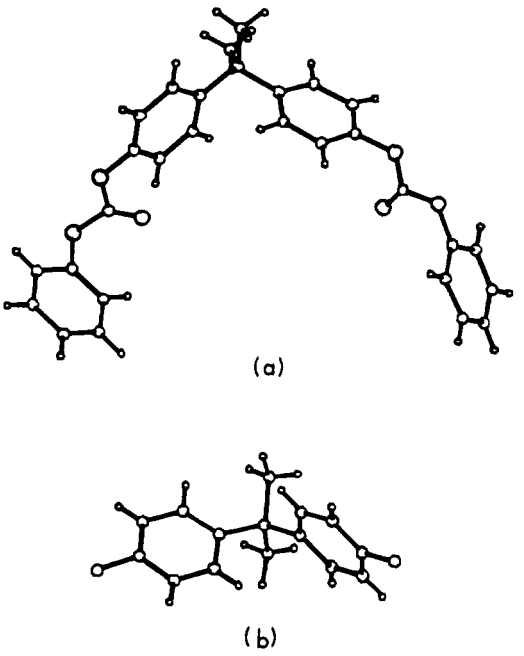

Figure 2. (a) View of the molecule of DPBC as found in the solid state. (b) Details of the spatial arrangement displayed at the isopropylidene junction of DPBC in the solid state.

Table IV
Bond Angles (Deg) and Their Estimated Standard Deviations

C(1)–O(1)–C(7) = 119.3 (2)	C(21)–O(6)–C(22) = 116.8 (2)
O(1)–C(7)–O(3) = 106.5 (2)	O(4)–C(21)–O(6) = 105.5 (2)
O(1)–C(7)–O(2) = 127.3 (2)	O(6)–C(21)–O(5) = 127.5 (2)
O(3)–C(7)–O(2) = 126.1 (2)	O(4)–C(21)–O(5) = 127.0 (2)
C(7)–O(3)–C(8) = 115.4 (2)	C(21)–O(4)–C(18) = 117.2 (2)
O(1)–C(1)–C(2) = 122.9 (3)	O(6)–C(22)–C(23) = 118.3 (4)
O(1)–C(1)–C(6) = 115.7 (2)	O(6)–C(22)–C(27) = 120.0 (3)
C(2)–C(1)–C(6) = 121.4 (3)	C(23)–C(22)–C(27) = 121.4 (4)
C(1)–C(2)–C(3) = 118.4 (3)	C(22)–C(23)–C(24) = 117.5 (6)
C(2)–C(3)–C(4) = 120.6 (3)	C(23)–C(24)–C(25) = 120.7 (6)
C(3)–C(4)–C(5) = 120.2 (3)	C(24)–C(25)–C(26) = 120.5 (5)
C(4)–C(5)–C(6) = 119.8 (4)	C(25)–C(26)–C(27) = 120.3 (6)
C(5)–C(6)–C(1) = 119.6 (3)	C(22)–C(27)–C(26) = 119.4 (5)
O(3)–C(8)–C(9) = 118.9 (2)	O(4)–C(18)–C(17) = 117.9 (3)
O(3)–C(8)–C(13) = 119.6 (2)	O(4)–C(18)–C(19) = 120.0 (2)
C(9)–C(8)–C(13) = 121.4 (2)	C(17)–C(18)–C(19) = 121.9 (2)
C(8)–C(9)–C(10) = 118.6 (2)	C(18)–C(17)–C(16) = 118.8 (3)
C(9)–C(10)–C(11) = 122.1 (3)	C(17)–C(16)–C(15) = 121.9 (3)
C(10)–C(11)–C(12) = 117.1 (2)	C(16)–C(15)–C(20) = 117.0 (2)
C(11)–C(12)–C(13) = 121.5 (2)	C(15)–C(20)–C(19) = 122.1 (3)
C(8)–C(13)–C(12) = 119.4 (2)	C(20)–C(19)–C(18) = 118.4 (2)
C(14)–C(11)–C(10) = 119.3 (2)	C(14)–C(15)–C(16) = 120.3 (3)
C(14)–C(11)–C(12) = 123.6 (2)	C(14)–C(15)–C(20) = 122.5 (3)
C(11)–C(14)–C(28) = 112.0 (2)	C(15)–C(14)–C(28) = 106.9 (2)
C(11)–C(14)–C(29) = 107.7 (2)	C(15)–C(14)–C(29) = 112.7 (2)
C(11)–C(14)–C(15) = 109.4 (2)	C(28)–C(14)–C(29) = 108.2 (3)

Table V
Torsion Angles (Deg) of Interest

C(2)–C(1)–O(1)–C(7) = –48.0	C(23)–C(22)–O(6)–C(21) = –102.4
C(6)–C(1)–O(1)–C(7) = 135.5	C(27)–C(22)–O(6)–C(21) = 82.7
C(1)–O(1)–C(7)–O(3) = –173.5	C(22)–O(6)–C(21)–O(4) = 177.5
C(1)–O(1)–C(7)–O(2) = 6.3	C(22)–O(6)–C(21)–O(5) = –1.2
C(8)–O(3)–C(7)–O(1) = –178.9	C(18)–O(4)–C(21)–O(6) = –170.9
C(8)–O(3)–C(7)–O(2) = 1.2	C(18)–O(4)–C(21)–O(5) = 7.7
C(9)–C(8)–O(3)–C(7) = 89.2	C(17)–C(18)–O(4)–C(21) = 89.0
C(13)–C(8)–O(3)–C(7) = –93.8	C(19)–C(18)–O(4)–C(21) = –96.5
C(10)–C(11)–C(14)–C(15) = –61.3	C(16)–C(15)–C(14)–C(11) = –35.9
C(12)–C(11)–C(14)–C(15) = 117.8	C(20)–C(15)–C(14)–C(11) = 148.8
C(10)–C(11)–C(14)–C(28) = –179.8	C(10)–C(15)–C(14)–C(28) = 85.7
C(10)–C(11)–C(14)–C(29) = 61.5	C(16)–C(15)–C(14)–C(29) = –155.8
C(12)–C(11)–C(14)–C(28) = –0.7	C(20)–C(15)–C(14)–C(28) = –89.7
C(12)–C(11)–C(14)–C(29) = –119.4	C(20)–C(15)–C(14)–C(29) = 28.9

Even though the molecule does not lie on a crystallographic symmetry element, the X-ray data reveal excellent agreement between the chemically identical parts of the molecule. The $C(sp^2)$–$C(sp^2)$ aromatic distances observed average 1.367 Å. The average $C(sp^2)$–H bond distance is 0.92 Å, while individual values range from 0.80 to 0.98 Å. The average bond angle for each of the six-membered rings is 120°, and all the angles involving the H atoms in the aromatic rings are consistent with sp^2 geometry.

In this structure, the carbonate group is planar and is found to be in a trans–trans conformation. A similar conformation was reported for diphenyl carbonate,[14] whereas a cis–trans orientation was found for the carbonate moiety of DPBC when complexed with a dye molecule.[1] The overall geometry is close to that occurring in aromatic esters. The C–O bond average is 1.328 Å. Because of its partial double-bond character, only small deviations (<10°) away from the planar conformation are expected to occur. Those found in this crystal structure are +6.5°, +1.1°, –9.0°, and +2.5°. Both C=O bonds are shorter (1.172 (3), 1.151 (3) Å) than the expected C=O bond distance of 1.21 Å. Such a strong double bond is thought to be responsible for the increase in the magnitude of O—C=O valence angles (mean value 127°), which is about 3° larger than the corresponding angles in aromatic esters. Consequently, a shrinkage of the C—O—C valence angle is observed (106°).

According to Erman et al.,[14] the relative orientation of the carbonyl group with respect to an adjacent phenyl group is determined by two opposing effects: steric interactions between the carbonyl oxygen atom and ortho C–H group of phenyl, which would favor a perpendicular arrangement (θ = 90°), and electron delocalization favoring a planar arrangement (θ = 0°, 180°). In the present work, we found that three of the four observed conformations correspond to a perpendicular type of arrangement (θ = 82.7°, 89.2°, 89.0°), whereas only one intermediate arrangement (θ = –48.0°) is found. The influence of the relative orientation of the carbonyl group with respect to the phenylene group shows up in a marked difference occurring between the two equivalent valence angles at the phenylene junction (see, for example, O(1)–C(1)–C(2) = 122.9 (3)° and O(1)–C(1)–C(6) = 115.7 (2)°). The energy associated with such an alteration can be estimated to be on the order of 2 kcal/mol. Figure 3 is a plot of the variation of the magnitude of this valence angle (defined as O–C–Cx) as a function of the nonbonded distance between ortho carbon atom Cx and the carbonyl oxygen atom O. It is clear that the opening of the valence angle occurs in order to relieve the short nonbonded contact Cx···O and Hx···O. An equilibrium is reached, e.g., having comparable magnitudes for the O–C–X angles, when the carbonyl bond lies perpendicular to the aromatic plane. The carbonate valence angles are apparently affected in a similar manner

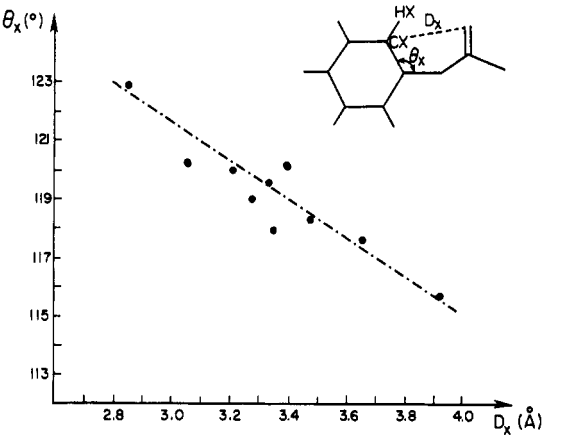

Figure 3. Plot of the variations of the valence angle Ox, as a function of the nonbonded distance between the carbonyl oxygen atom and the ortho carbon atom Cx. The points are drawn from the present study and other works dealing with comparable molecular fragments.

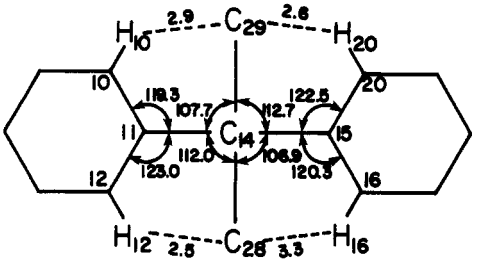

Figure 4. Fischer projection of the observed geometry around C(14) in the crystal structure of DPBC. Correlations among the various valence angle deformations and the short nonbonded contacts H(20)···C(29) and H(12)···C(28) are apparent. See text for discussion.

(e.g., compare C(1)–O(1)–C(7) to C(8)–O(3)–C(7)).

The relative orientation of two adjacent phenylene rings may be described by torsion angles Φ and Ψ about the C(11)–C(14) and C(14)–C(15) bonds, respectively. The particular conformation found in crystalline DPBC is such that each methyl carbon atom lies, or almost lies, in the plane of one of its adjacent phenyl rings (Figure 2b). This arrangement is responsible for the lack of elongation observed for the molecule. The orientation found for the methyl hydrogen atoms is close to the stable combination of trans, gauche$^+$, gauche$^-$ orientations, with respect to the two $C(sp^3)$–$C(sp^3)$ bonds of the linkage.

The average valence separations and angles around C(14) are normal at 1.533 Å and 109.5°, respectively, but chemically equivalent angles differ by as much as 7°, which is well outside experimental error and must be considered a real effect. These valence angle deformations are apparently related to interactions between the phenyl groups and the methyl groups. Figure 4 clearly indicates that the expansion of the C(15)–C(14)–C(29) angle is caused by the short contact between H(20) and C(29), which is 0.3 Å less than the carbon–hydrogen van der Waals radii sum. A similar interaction between H(10) and C(29) is responsible for the expansion of C(11)–C(15)–C(20). The deformations also extend to the phenylene groups where the nonequivalence of C(14)–C(15)–C(20) and C(14)–C(15)–C(16) also results from the crowding of H(20) and C(29). A similar asymmetry is observed for the other ring in the angles around C(11). It should be noted that none of the methyl group hydrogen atoms are involved in nonbonded separations less than the appropriate intermolecular radii sum. Since nonbonded distances of the type H(20)···C(29) are

Table VI
Intermolecular and Packing Features of the DBPC Crystal Structure

molecules[a]	intermolecular energy, kcal/mol	no. of short contacts[b]
I + *b*	-3.64	48
I - *b*	-3.64	48
II + *a* + *c*	-3.12	41
II + *a* - *b* + *c*	-3.12	41
II + *a*	-2.66	35
II + *a* - *b*	-2.66	35
I + *c*	-2.37	31
I - *c*	-2.37	31
II - *c*	-2.16	28
II - *b* - *c*	-2.16	28
II + *a* - *b*	-1.54	21
II + *a* + *b*	-1.54	21

[a] I: x, y, z; II: $-x, {}^1/_2 + y, -z$. [b] A short contact is defined as two atoms separated by less than 1.5 times the sum of their respective van der Waals radii.

a strong function of the torsion angles Φ and Ψ, the valence deformations around C(14), C(15), and C(11) will also be correlated to these rotations.

The intermolecular arrangement found in the crystal structure is consistent with a highly dense packing, since each DPBC molecule is surrounded by 12 neighbors. In order to arrive at a full description of the packing arrangement, the intermolecular energy between a given molecule, i.e., the reference molecule and all its neighbors, was evaluated by taking into account the nonbonded interactions. These calculations, which are summarized in Table VI, were performed by using the same parameters as those utilized in the conformational analysis of the single molecule. Also, the number of "short" contacts, corresponding to interatomic distances less than 1.5 times the sum of the van der Waals radii of the interacting atoms, are reported. It can be seen that the strongest cohesion occurs between the reference molecule and its equivalents, as derived from a translation along the *b* axis (Figure 5a), which is the shortest axis. Incidentally, the morphology of the crystals is such that they develop preferentially along this direction. The remainder of the intermolecular interactions occurs between molecules lying in the (*a*, *c*) plane (Figure 5b). At this point, it should be noted that the phenyl ring which deviates from a perpendicular arrangement with respect to its adjacent carbonate group ($\theta = -48°$) exhibits an orientation whereby it lies almost parallel to phenyl rings from neighboring molecules. This suggests that the observed departure from the $\theta = 90°$ conformation arises, at least in part, from intermolecular interactions peculiar to the crystal.

B. Conformational Analysis of the Polycarbonate BPAPC. In the following study, the diphenyl carbonate moiety is considered as the monomeric unit, the junction between two contiguous repeating units being at the isopropylidene group.

Since the crystal structure results for DPBC show significant valence angle distortions resulting from intramolecular nonbonded interactions peculiar to the values of Φ, Ψ, and θ found in the crystal, the valence parameters used in this study were derived by averaging the appropriate observed quantities to restore the monomeric unit to a symmetrical, unstrained state. The results of this averaging process are given in Figure 6. Furthermore, in order to model the polymer chain, a quaternary carbon atom was generated at the para position of the terminal phenyl ring. The distance between this atom and the quaternary carbon atom at the isopropylidene linkage will be referred to as the virtual bond (*L*).

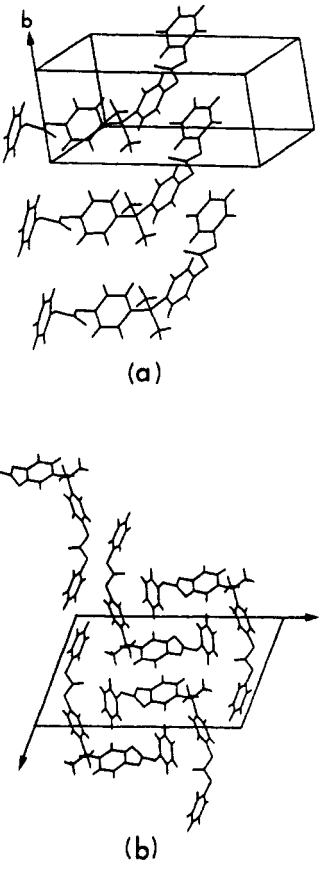

Figure 5. Packing in crystalline DPBC. (a) Molecules related by translations along the *b* axis. (b) Projection in the (*a*, *c*) plane.

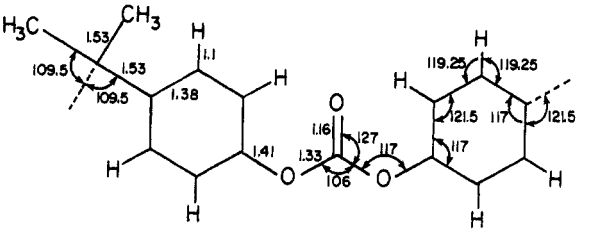

Figure 6. Bond parameter values of the monomeric unit used for conformational calculations on BPAPC. These values were obtained by averaging chemically equivalent quantities from the crystal structure of DPBC reported in this work.

The main purpose of the present calculations is to investigate the influence of the backbone torsion angles on the conformation of the molecule. However, several calculations involving valence angle deformations of the isopropylidene group will also be described.

Evidence showing the carbonate group to be predominantly planar is well supported by structural work. The partial double-bond character of the C–O bond of the carbonate group, as shown by a shortening of about 0.10 Å, appears to be responsible for the planarity of this group. For a group such as

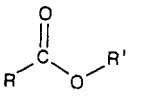

where R is not an oxygen atom, the trans form is predicted over cis, due to steric repulsion between R and R′ in the cis conformation. When R is an oxygen atom, quite a different situation may arise due to the peculiarity of the O–C–O–R′ sequence. For example, in the case of carbohydrate molecules where the C–O–C–O–C sequence is

found, the trans conformation is not the stable one. This feature is commonly thought to arise from dipolar interactions involving the lone-pair electrons of neighboring oxygen atoms. Furthermore, experimental evidence from the crystal structure of DPBC cocrystallized with a dye molecule[2] shows that the cis–trans conformation of the carbonate moiety can be isolated. For these reasons, both trans–trans and cis–trans conformations will be considered. Because of the partial double-bond character of the C–O bond, only small deviations (<10°) away from these planar conformations have to be considered. The torsion angles θ_1 and θ_2 describe the relative orientation of the carbonate group with respect to the adjacent phenylene groups. As discussed above, a perpendicular arrangement seems to be preferred and will be used as the reference value in this work. Nevertheless, deviations of 45° away from this orientation have been observed,[19] and their effect will be discussed.

From these considerations, the conformations of the monomeric unit will initially be restricted to the following values of the torsion angles: θ_1 = [−90, 90], ω_1 = [0, 180]; ω_2 = [0, 180], θ_2 = [−90, 90]. The number of starting models to be examined can be reduced further due to (i) the fact that a cis–cis conformation of the carbonate moiety about torsion angles ω_1 and ω_2 is precluded by severe overlap of the adjoining phenylene rings and (ii) the symmetry of the phenylene rings and carbonate groups is such that only one of the four possible combinations of θ_1, θ_2 is unique.

This point is only of importance for the helical parameter analysis, since the conformations of the carbonate groups are expected to have a negligible effect on the conformation around the isopropylidene group. Therefore, as far as conformations of this monomeric unit are concerned, only two need to be described. The first one is obtained for a trans–trans conformation of the carbonate sequence and has a nonbonded energy of 0.4 kcal/mol. The length of the virtual bond is 12.34 Å and corresponds to the maximum elongation of that monomeric unit. Introducing a cis–trans conformation within the carbonate sequence results in a monomeric unit having a total extension of 10.69 Å and an energy of 1.3 kcal/mol.

It has been stated by a number of workers[14-16] that the cis–trans conformation is considerably less stable than the trans–trans conformation of the carbonate. However, the calculated energy differences favoring the trans–trans conformation (1.3[17] and 1.8 kcal/mol[15]) are comparable to our value of 0.9 kcal/mol, given that different potential parameters and valence geometries were used in these studies. Although an energy difference of ~1 kcal/mol may be sufficient to favor the trans–trans conformation in solution, the magnitude of intermolecular interactions in the solid could compensate for this difference (cf. Table VI). In fact, the molecule reported here has been observed[1] in the all-(cis–trans) conformation in a cocrystalline complex of DPBC and a dye molecule.

Within the selected scheme of energy functions, both conformations may be considered as comparable. As previously stated, these different conformers were generated for discrete values of torsion angles θ and ω. Several other models were generated for values of these torsion angles consistent with the limit of variations expected. No significant variations of the energy were found. The length of the virtual bond was found to be strikingly constant (variations of the order of 0.05 Å). Such an invariance results from the fact that rotations (θ_1 and θ_2) about the C–O bond connecting the carbonate group to the adjoining rings occur along the main axis of the phenylene rings and has little bearing on the location of the quaternary carbon atoms defining the virtual bond.

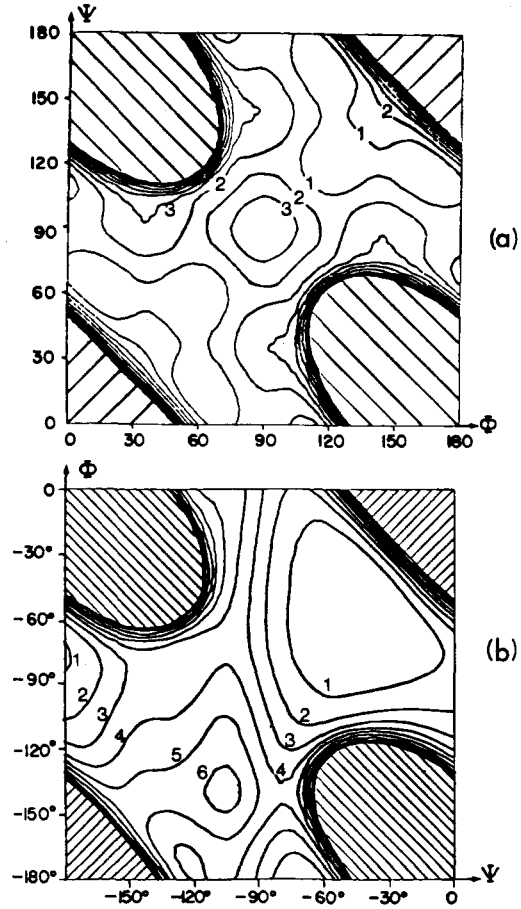

Figure 7. Energy contour plots as a function of the rotation angles Φ and Ψ. Contours are drawn at 1 kcal/mol intervals relative to the minimum and regions with diagonal lines are at energies >10 kcal/mol above the minimum. (a) All valence angles at the isopropylidene junction were fixed at tetrahedral values and all methyl group hydrogen atoms were in the staggered arrangement. (b) All valence angles around the isopropylidene group and all methyl group hydrogen atoms were fixed in the positions observed in the crystal structure of DPBC reported in this work (Tables III and IV).

Starting from the mean geometry derived from the crystal structure for the monomeric unit (Figure 6), another unit was constructed in the conventional fashion for rigid-bond transformations by using a valence angle C(11)–C(14)–C(15) of 109.5°. Such an approach implies that contiguous monomeric units in the polymer chain are in the same conformation. Then the energy occurring between two of these monomer units and the resulting helical parameters were computed as a function of the rotations about Φ and Ψ torsion angles. For obvious symmetry reasons, the isoenergy map does not have to be computed for the full angular range of Φ and Ψ torsion angles; however, this is not the case for the helical parameters.

Figure 7a was computed for Φ and Ψ ranging from 0 to 180° in 5° increments. The methyl group hydrogen atoms were in the staggered arrangement with respect to the isopropylidene C–C bonds. All valence angles for the isopropylidene group were fixed at 109.5°. It is obvious that rotations about Φ and Ψ are not subject to strong restrictions, since almost 40% of the total available space corresponds to conformations for which the nonbonded energy is within 4 kcal/mol of the minimum; the minimum occurs at (Φ, Ψ) = (60°, 20°) and (20°, 60°). The points (60°, 60°) and (60°, 40°) are 0.05 and 0.62 kcal/mol above

Table VII
Nonbonded Energies as a Function of Valence Angle Deformations

C(28)–C(14)–C(29)	C(11)–C(14)–C(15)	C(11)–C(14)–C(28) C(11)–C(14)–C(29) C(15)–C(14)–C(28) C(15)–C(14)–C(29)	energy min (Φ, Ψ)	ΔE, kcal/mol (60°, 60°)	(90°, 90°)	(60°, 40°)	(90°, 0°)
109.5°	109.5°	109.5°	(60°, 20°) (20°, 60°)	0.0	4.0	0.0	1.4
108.0°	109.5°	109.85°	(60°, 60°)	0.0	3.1	0.6	1.2
108.0°	108.0°	110.25°	(60°, 60°)	0.0	3.2	0.5	1.7
108.0°	111.0°	109.5°	(60°, 10°) (10°, 60°)	0.3	3.3	1.0	1.0
107.0°	112.0°	109.5°	(60°, 10°) (10°, 60°)	0.5	3.1	1.3	0.8
107.0°	107.0°	110.75°	(60°, 60°)	0	2.9	0.7	2.0

Table VIII
Nonbonded Energies as a Function of Methyl Group Rotations

(Φ, Ψ)	energy min (χ_1, χ_2)[a]	$\Delta E(\chi_1 = \chi_2 = 60°)$,[b] kcal/mol
(60°, 60°)	(60°, 60°)	0.0
(90°, 90°)	(60°, 60°)	0.0
(60°, 40°)	(60°, 70°)	0.9
(90°, 0°)	(50°, 70°)	1.7

[a] The torsion angles χ_1 and χ_2 are defined as follows: χ_1 = H(281)–C(28)–C(14)–C(29); χ_2 = H(291)–C(29)–C(14)–C(28). $\chi_1 = \chi_2 = 60°$ represents the ideal staggered arrangement of the methyl groups. [b] An inherent threefold torsion potential with a barrier of 3 kcal/mol was included in all calculations.

the minimum, respectively. Table VII summarizes a number of similar calculations for which the valence geometry of the isopropylidene group was distorted in such a way that the angles C(11)–C(14)–C(28), C(11)–C(14)–C(29), C(15)–C(14)–C(28), and C(15)–C(14)–C(29) were all equal. Although the position of the minimum varies considerably, all maps are quite similar. Therefore, small changes of this type in the valence angles around C(14) do not give rise to large changes in the nonbonded energy. In all cases, the point (90°, 90°) is less than 4 kcal/mol from the minimum. In Table VIII, selected values of Φ and Ψ were used, and rotations of the methyl groups were investigated. An inherent threefold torsion potential of 3 kcal/mol was assumed for rotations about the C(14)–C(28) and C(14)–C(29) linkages. For symmetrical arrangements of the phenyl groups, the minimum of energy is not displaced from the ideal staggered arrangement. For unsymmetrical phenyl group arrangements, the minimum for the methyl group rotations is displaced. The energy associated with methyl group relaxation did not exceed 1.7 kcal/mol for the points investigated.

Figure 7b was calculated with all bond lengths and angles as observed in the crystal structure of DPCB (Tables II and III). Comparison of parts a and b of Figure 7 shows that the valence angle deformations depicted in Figure 4 distort the symmetry of the map, and the point (−60°, −40°) is now the minimum. This should be compared to the observed conformation (−61°, −36°) from Table V. Investigation of the methyl group rotations using the observed isopropylidene valence geometry and fixing (Φ, Ψ) at (−61°, −36°) indicated that the observed methyl group arrangement is already very close to the minimum of energy.

It would seem then that the isopropylidene group can respond in two distinct ways to an unsymmetrical arrangement of the phenyl groups: by methyl group rotations and by valence angle deformations. The importance of the methyl group rotations was pointed out previously,[16,19] but, if the crystal structure results reported here can be taken as a general indication, C–C–C valence angle deformations may, in fact, be preferred.

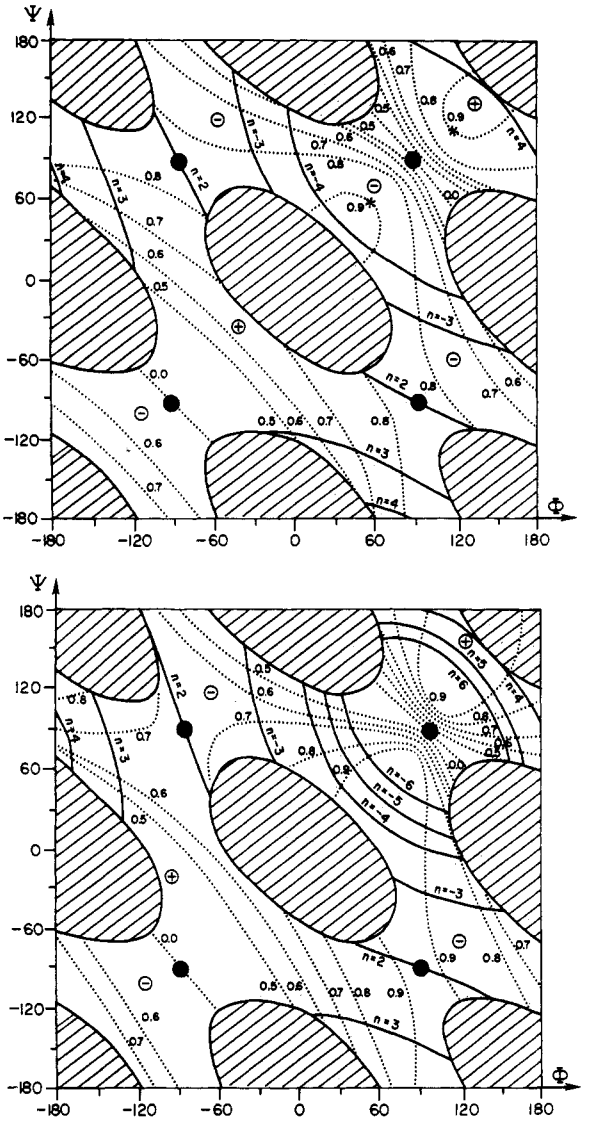

Figure 8. Variations of the helical parameters as a function of rotation angles Φ and Ψ. Regions with diagonal lines are at energies >10 kcal/mol from the minimum. (—) iso-n contours; (···) iso-h contours expressed as a fraction of L, the virtual bond length; circled pluses and minuses indicate zone chirality. (a) Trans–trans conformation, L = 12.34 Å. The values of the fixed torsion angles are $\theta_1 = 90°$, $\omega_1 = 180°$, $\omega_2 = 180°$, and $\theta_2 = 90°$. (b) Cis–trans conformation, L = 10.69 Å. The values of the fixed torsion angles are $\theta_1 = -90°$, $\omega_1 = 180°$, $\omega_2 = 0°$, $\theta_2 = 90°$.

The helical parameters (n, h) were computed for the full angular range of Φ and Ψ at 10° intervals. Figure 8a represents a plot of the variations of the helical parameters calculated with the carbonate moiety being in a trans–trans

Table IX
Selected Helical Parameters

θ_1	ω_1	ω_2	θ_2	(Φ, Ψ) (−90°, −90°)	(−90°, +90°)	(+90°, −90°)	(+90°, +90°)
90°	180°	180°	90°	n = 2.87	n = 2	n = 2	n = 1
				h = 0	h = 10.07	h = 10.07	t = 12.23
−90°	180°	180°	90°	n = 2	n = 2.87	n = 1	n = 2
				h = 10.07	h = 0	t = 12.23	h = 10.07
90°	0°	180°	90°	n = 2	n = 1	n = 2.60	n = 2
				h = 7.43	t = 10.69	h = 0	h = 9.72
−90°	0°	180°	90°	n = 1	n = 2	n = 2	n = 2.60
				t = 10.69	h = 7.43	h = 9.72	h = 0
−90°	180°	0°	90°	n = 2.60	n = 2	n = 2	n = 1
				h = 0	h = 7.43	h = 9.72	t = 10.69
−90°	0°	180°	−90°	n = 2	n = 2.60	n = 1	n = 2
				h = 9.72	h = 0	t = 10.69	h = 7.43

conformation. Figure 8b gives the helical parameters corresponding to the cis–trans conformation. The contours corresponding to iso-h values are given as a fraction of the maximum elongation as determined by the magnitude of the virtual bond, L. From these plots, it is striking to see how the polymer can display various architectures ranging from the cyclic kind of structure to the totally extended shape. All these architectural features occur for conformations belonging to the low-energy region of the map. Moreover, the interconversion between these different forms, i.e., topological rearrangements, can occur in a continuous fashion requiring cooperative rotations about Φ and Ψ. Such conformational and architectural flexibilities, which are not found for the common polyesters, may explain the particularly remarkable mechanical properties of biphenyl polycarbonates. Undoubtedly, consideration of the dispersion of n and h values provides an explanation of the difficulty encountered in the preparation of highly crystalline oriented samples of biphenyl polycarbonates. The analysis also reveals that the observed crystallographic conformation of DPBC would generate a polymer chain having n = 2.45 and h = 7.10 Å. The map presented in Figure 7a is similar to those reported by Erman et al.,[14] Tekely and Turska,[15] and Sundararajan.[16]

To facilitate discussion of polycarbonate chains in the crystalline phases, we have made a number of helical parameter calculations assuming values of Φ and Ψ = ±90°. The helical parameters were evaluated for these four discrete conformations about Φ and Ψ and the six other combinations of ω_i and θ_i. The results listed in Table IX show that there are a number of symmetry-equivalent sets of θ_1, θ_2, ω_1, and ω_2 due to the symmetry of the phenylene and carbonate groups.

It should be noted, that, for a given monomeric conformation, several helical architectures are generated as a function of Φ and Ψ. The occurrence of cyclic structures is indicated by values of h = 0. Such structures are not compatible with arrangements of macromolecular chains but may be considered as models for chain folding. However, the cyclic oligomers occurring in the quadrant ($0 \le \Phi \le 180, 0 \le \Psi \le 180$) are qualitatively different from those occurring in the quadrant ($-180 \le \Phi \le 0, -180 \le \Psi \le 0$). Cyclic structures in the negative quadrant contain a small number of monomers (<5) and represent quite contracted conformations with respect to the total elongation possible for two contiguous monomers. On the other hand, cyclic oligomers in the positive quadrant contain a large number of monomers per turn (>15) and range from quite extended to the most greatly extended conformation possible. Thus, these conformations are not too far removed from being simple translation chains. In particular, if one increased the C(11)–C(14)–C(15) valence angle by 2.5°, the point (Φ = 90°, Ψ = 90°) corresponds to a simple translation chain with an identity period of 10.7 Å for the cis–trans conformation of the carbonate group.

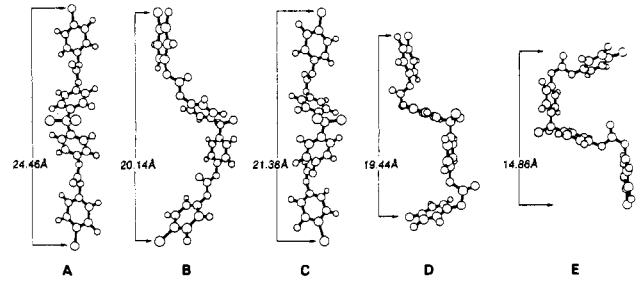

Figure 9. Representation of five idealized conformations of two contiguous monomeric units of BPAPC (see text for discussion). Terminal methyl groups and central methyl hydrogen atoms have been omitted. A and B correspond to a trans–trans conformation of the carbonate moiety (θ_1 = 90°, ω_1 = 180°, ω_2 = 180°, θ_2 = 90°) with the pair of torsion angles (Φ, Ψ) equal to (+90°, +90°) and (+90°, −90°), respectively. C, D, and E are obtained for a cis–trans conformation of the carbonate moiety (θ_1 = −90°, ω_1 = 180°, ω_2 = 0°, θ_2 = +90°), the conformation at the isopropylidene linkage being (Φ = +90°, Ψ = +90°) for C, (Φ = +90°, Ψ = −90°) for D, and (Φ = −90°, Ψ = +90°) for E.

Moreover, it should be understood that the helical parameter maps reported here use only two independent torsion angles about the isopropylidene junction, whereas the fiber data (see below) for crystalline BPAPC allows for four such crystallographically independent torsion angles. Clearly, one could construct a number of simple translation chains (or glide-type chains) with this increase in the number of degrees of freedom. They would all be similar to the conformations characterized by the h = 0 line in the positive quadrants (Figure 8). For simplicity of notation in the discussions that follow, we refer to these chains as simple translation chains even though they would require some adjustment of the valence geometry or a greater number of independent torsion angles to become so.

Two sets of Φ and Ψ values give rise to two twofold helical structures (n = 2). One combination of Φ and Ψ induces a pure translation of the monomeric units along the chain axis. Examination of the 24 possible helical arrangements so obtained discloses that only five among them need be considered in reference to crystalline polycarbonates (Figure 9). Again, it should be stressed that these models represent five different types of helical arrangements, but slight variations away from these idealized structures are likely. In particular, it should be pointed out that, although the conformations characterized by (Φ, Ψ) = ±90° represent special limiting helical structures (given the fixed reference values of θ_1 and θ_2), they also occur at a local point of maximum energy in the low-energy regions of the map. Therefore, one would not expect these

precise conformations to occur in the solid state.

The foregoing has been based on reference values of (θ_1, θ_2) = ±90°, which describe a perpendicular arrangement of the planes of the phenylene groups relative to those of the carbonate groups. Assuming a symmetrical geometry for the phenylene rings, the atoms C(14), C(11), C(8), and O(3) fall on a straight line. With this condition (and similarly for the other ring), the helical parameters, given fixed values of ω_1 and ω_2, are only a function of the torsion angles τ_2 = C(14)–O(3)–C(7)–O(1) and τ_1 = C(14′)–O(1)–C(7)–O(3). (C(14′) is the isopropylidene carbon atom that would be attached to C(4) in the polymer.) These torsion angle definitions are a bit unusual since, for example, C(14) and O(3) are not connected by a valence bond, but, due to the linearity of the phenylene groups, these definitions are quite useful. In terms of the previously defined angles, $\tau_1 = \Psi + \theta_1$ and $\tau_2 = \Phi + \theta_2$. Thus, for any fixed values of the θ_1 and θ_2, a helical parameter map over the full range of Φ and Ψ will also cover the full range of τ_1 and τ_2. Therefore, the maps shown in Figure 8 display the full range of helical conformations of the polymer despite the fact that θ_1 and θ_2 were fixed. The origin of maps displayed in the (τ_1, τ_2) system would, of course, be shifted by θ_1 and θ_2, respectively, from those in Figure 8.

The process of relating an energy map to the helical parameter maps is a somewhat different matter. In order to obtain a full description of the chain energetics, one must not only consider rotations about Φ and Ψ as we have done but one must also consider the energetics of rotations about θ_1 and θ_2. The valence angle deformations described above notwithstanding, the main obstacle to making such a calculation is to estimate the energy associated with delocalization between the carbonate group and the phenylene rings. Normally, one models this type of effect by including an inherent twofold torsion potential for the rotation and treating the nonbonded interactions in the usual manner. If the following functional form for the torsion potential is chosen

$$V = -V_0 \cos^2(\theta)$$

the maximum stabilization due to delocalization is V_0. The problem is then reduced to finding a value for V_0. Sundararajan[16] has estimated V_0 to be 6–8 kcal/mol by assuming the total potential (delocalization + nonbonded) reaches a minimum at θ = 45°, which is the value observed for crystalline diphenyl carbonate.[14] This approach is not, however, completely satisfactory because intermolecular nonbonded interactions can have a rather large effect on phenyl rotations in the solid state. For example, V_0 for biphenyl is 9.0 kcal/mol and the minimum for the total potential is calculated to occur at θ = 40°, in good agreement with gas-phase electron diffraction data.[18] However, a value of θ = 0 is observed in crystalline biphenyl.[19] Examples where θ is larger than expected have also been observed in crystalline solids.[20] Nevertheless, it is possible to extract delocalization parameters from crystal data, but one must take into account both intramolecular and intermolecular nonbonded interactions by minimizing the total crystal energy. This approach has yielded good results for the case of crystalline bitolyl,[20] but this is beyond the scope of this work.

In the absence of a value for the delocalization parameter, it is not possible, for example, to find what values of Φ, Ψ, θ_1, and θ_2 correspond to the minimum-energy arrangement of a helical structure characterized by τ_1 and τ_2. For this reason, we have not superimposed any of the fine details of the energy map (Figure 7a) on the helical parameters maps (Figure 8). However, the following qualitative considerations should suffice in obtaining a general understanding of the effects of variations in θ_1 and θ_2 away from the reference values used in this work. Let us assume that the total potential (delocalization and nonbonded) for θ reaches a minimum at ±60° and ±120°, instead of ±90° as would be the case for V_0 = 0. Then a chain with Φ = 60°, θ_1 = 120°, Ψ = 60°, and θ_2 = 120° would be close to the energy minimum but would have the same helical parameters as a chain with $\Phi = \Psi = \theta_1 = \theta_2$ = 90°. Thus, for any particular values of θ_1 and/or θ_2 different from 90°, the origin of the helical parameter map in Figure 8 would be shifted along the Φ and Ψ axes by amounts corresponding to θ_1 and θ_2, respectively, and the relative energies of various helical structures would change. Should data on the delocalization parameter for this system become available, the most straightforward approach would be to recalculate the helical parameter maps with new reference values for θ_1 and θ_2.

Table X
Summary of the Crystal Data for Polycarbonates[a]

	>C(CH$_3$)$_2$		–S–	>CH$_2$
a, Å	11.9	12.3	5.6	5.0
b, Å	10.1	10.1	8.7	10.5
c, Å	21.5	20.8	22.2	22.0
β, deg	90.0	84.0	90.0	90.0
d, Mg m^{-3}	1.30	1.315	1.50	1.303
no. of monomers per cell	8	8	4	4
ref	21	22	22	22

[a] The fiber axis is chosen to coincide with the crystallographic c axis.

C. Comparison with Experimental Results. Since all the calculations have been carried out on general grounds, the predictions are expected to describe and cover the range of conformations observed for the polymer and its model compounds.

As for polycarbonates, two sets of crystal data derived from X-ray fiber diffraction patterns have been reported for BPAPC.[21,22] Lattice constants of polycarbonates from bis(4-hydroxyphenyl)methane and bis(4-hydroxyphenyl) sulfide have also been reported.[22] The proposed structural models for the crystalline polymers derived from these studies have not been tested extensively. Full structure factor calculations have not been reported, and no attempt has been made to calculate the cohesive energy of the crystals. Table X summarizes the cell data for polycarbonates.

In the case of the polycarbonate from BPAPC, the inconsistency observed for the magnitude of the fiber repeat (21.5[21] and 20.8 Å[22]) can be accounted for by the lack of a strong meridional reflection on the fiber diffraction diagrams. The crystal is reported to have two independent chains per cell and two chemical repeats per fiber repeat. This limits the possible chain conformations to be either 2_1 helices, glide-type chains or simple translation chains with two independent monomers per repeat. From our calculations, it seems unlikely that any of the chains exhibiting 2_1-helical symmetry are capable of matching the observed fiber repeat. Even the 2_1 helix with the trans–trans conformation of the carbonate group (Figure 9, model B) would require a valence angle expansion of ca. 5.5° in order to match the observed repeat. For pure translational symmetry and the two monomeric units having a trans–trans arrangement of the carbonate moieties, the fiber repeat represents a significant contraction relative to the maximum extension of the chain. On the other hand, when a cis–trans arrangement of the carbonate moiety is considered (maximum extension of two residues = 21.38 Å), only a small contraction would be sufficient to match the observed fiber repeat. As noted earlier, these contractions

can be achieved via torsion angle adjustments since the fiber repeat contains two independent sets of such angles.

As for the polycarbonate from bis(4-hydroxyphenyl)-methane and bis(4-hydroxyphenyl) sulfide, it is clear that only the trans–trans arrangement of the carbonate moieties and a pure translation of the monomeric unit can accommodate the observed fiber repeats. In this case, a shrinkage of about 10% would be required.

The fact that the polycarbonate of BPAPC forms a cocrystalline complex that is similar in structure to the cocrystalline compound formed by DPBC[1] can be discussed from two points of view. If one were to argue that the aggregation process depends upon the conformation of the polymer in the crystalline phase, then as discussed above, there are only two possible chain conformations given the observed fiber repeat (Table VIII) and the calculated helical parameter maps. These are models A and C (Figure 9), and it should be pointed out that model C is very similar to the conformation observed in the model aggregate structure.[2] With respect to the conventions used in the present work, conformation of the DPBC molecule found in the model aggregate structure[1] is described by $\theta_1 = 104°$, $\omega_1 = -2°$, $\omega_2 = 172°$, $\theta_2 = 97°$, $\Phi \simeq -96°$, $\Psi \simeq 80°$; this yields an extension of 21 Å for the fiber repeat.

If, on the other hand, aggregation depends upon the chain conformations occurring in the less-ordered regions of polymer film, one would initially consider each of the five idealized models in Figure 9 on an equal basis. However, contracted conformations such as models D and E would not be expected to pack well either with similar polymer segments or with the dye chains and should not be present in a dense polymer film to any great extent. In any case, there is a definite and relatively small number of chain models that one would have to consider as potential periodic templates for the aggregation process.

Acknowledgment. We thank Dr. P. R. Sundararajan for providing the results of his energy calculations prior to publication.

Registry No. DPBC, 20325-64-8; BPAPC (copolymer), 25037-45-0; BPAPC (SRU), 24936-68-3.

Supplementary Material Available: Table A, thermal parameters for DPBC (2 pages); Table B, observed and calculated structure factor amplitudes (13 pages). Ordering information is given on any current masthead page.

References and Notes

(1) Dulmage, W. J.; Light, W. A.; Marino, S. J.; Salzberg, C. D.; Smith, D. L.; Staudenmayer, W. J. *J. Appl. Phys.* **1978**, *49*, 5542.
(2) Borsenberger, P. M.; Chowdry, A.; Hoesterey, D. C.; Mey, W. *J. Appl. Phys.* **1978**, *49*, 5555.
(3) (a) Kercha, Yu. Yu.; Lipatov, Yu. S.; Moisya, Ye. G.; Pasechnik, Yu. V.; Savchenko, R. L. *Vysokomol. Soedin., Ser. A* **1971**, *A13*, 1986. (b) Moisya, E. G.; Semenovich, G. M. *Opt. Spectrosc. (Engl. Transl.)* **1970**, *29*, 324 [*Opt. Spektrosk.* **1970**, *29*, 607].
(4) (a) Parikh, D.; Phillips, P. J. *J. Chem. Phys.* **1985**, *83*, 1048. (b) Parikh, D.; Phillips, P. J. *J. Chem. Phys.* **1986**, *89*, 545.
(5) Chandhuri, N. K.; Aravindanath, S.; Betrabet, S. M. *J. Polym. Sci., Polym. Lett. Ed.* **1981**, *19*, 131.
(6) Main, P.; Fiske, S. J.; Hull, S. E.; Lessinger, L.; Germain, G.; Declercq, J. P.; Woolfson, M. M. "Multan 82, A System of Computer Programs for the Automatic Solution of Crystal Structures from X-Ray Diffraction data"; University of York: York, England, 1982.
(7) IUPAC–IUB Commission of Biochemical Nomenclature *Arch. Biochem. Biophys.* **1971**, *145*, 7. *J. Mol. Biol.* **1970**, *52*, 1.
(8) Scott, R. A.; Scheraga, H. A. *J. Chem. Phys.* **1966**, *45*, 2091.
(9) Gagnaire, D.; Perez, S.; Tran, V. H. *Carbohydr. Res.* **1980**, *78*, 89.
(10) Perez, S.; Scaringe, R. P. *J. Appl. Cryst.* **1986**, *19*, 65.
(11) Perez, S.; Scaringe, R. P. "INTPAK: An Interactive Computer Program for Intermolecular Energy Calculation", unpublished.
(12) Perez, S. "Programmes Interactifs de Generation d'Entites Moleculaires"; CERMAV (CNRS): Grenoble, France, 1980.
(13) Perez, S. "PHIPSI: Programme de Calcul d' Energie"; CERMAV (CNRS): Grenoble, France, 1980.
(14) Erman, B.; Marvin, D. C.; Irvine, P. A.; Flory, P. J. *Macromolecules* **1982**, *15*, 664.
(15) Tekely, P.; Turska, E. *Polymer* **1983**, *26*, 667.
(16) Sundararajan, P. R. *Can. J. Chem.* **1985**, *63*, 103.
(17) Williams, A. D.; Flory, P. J. *J. Polym. Sci.* **1986**, *6*, 1945.
(18) Dashevsky, V. G.; Kitaijorodsky, A. I. *Theor. Exp. Chem. (Engl. Transl.)* **1967**, *3*, 22 [*Theor. Eksp. Khim.* **1967**, *3*, 43] and references therein.
(19) Casolone, G.; Mariani, C.; Mugnoli, A.; Simonetta, M. *Mol. Phys.* **1968**, *5*, 339.
(20) Williams, D. E. *Acta Crystallogr., Sect. A* **1972**, *A28*, 629.
(21) Prietschk, A. *Kolloid-Z.* **1958**, *156*, 8.
(22) Bonart, R. *Makromol. Chem.* **1966**, *92*, 149.